Scientific Visualization, 2022, volume 14, number 5, pages 96 - 107, DOI: 10.26583/sv.14.5.07

Accurate 3D Visualization of Real Flow in Aerodynamic Study

V. A. Knyaz[1,A,B], V. V. Kniaz[2,A,B], M.M. Novikov[3,C], E.V. Ippolitov[4,C]

[A] Moscow Institute of Physics and Technology
[B] State Research Institute of Aviation System
[C] Institute on Laser and Information Technologies of RAS – branch Research Centre Crystallography and Photonics RAS

[1] ORCID: 0000-0002-4466-244X, knyaz@gosniias.ru
[2] ORCID: 0000-0001-7116-9338, vl.kniaz@gosniias.ru
[3] ORCID: 0000-0003-0626-793X, novikov@rambler.ru
[4] ORCID: 0000-0002-0622-6727, ippevg@yandex.ru

Abstract

Physical flow modelling is a powerful tool in aerodynamic researches, especially in analysis of complicated and dangerous conditions. It allows to study flow behaviour and to obtain reliable results via similitude concept, that is widely used in aerodynamics and hydrodynamics. Visualization of flow jets is one of the basic tools for analysis of flow behaviour under different flying conditions. Optical registration and 3D measurement techniques extend the capacities of visual flow study, providing both qualitative and quantitative data. The presented study addresses the problem of development of the vision-based technique for accurate flow 3D registration and 3D visualization. Algorithms allowing accurate 3D reconstructing of flow jets are presented, along with discussion of application for experimental flow 3D visualization.

Keywords: aerodynamic flow visualization, optical 3D measurements, refraction, calibration, accuracy.

1 Introduction

The practice of aero and hydrodynamic researches widely exploits physical models of flow in aerodynamic and hydrodynamic tunnels, that allow obtaining aerodynamic forces and momentums for various flow velocities and aircraft evolutions. The similitude concept serves as the basis for establishing correct conditions of an experiment to obtain results that are adequate to real flight. The similitude concept is based on correspondence of several dimensionless parameters of flow (Reynolds number, Mach number, Prandtl number and some others). The equivalence of these dimensionless parameters provide justification for results obtained in real and simulated environments. Based on similitude concept, aerodynamic process can be studied in hydrodynamic tunnel that allows taking the advantage of studying flow at low velocities.

Another part of aerodynamic research is to obtain reliable information about the characteristics of the flow and its behaviour in various flight conditions. And the visualization of the stream plays a very important role in this field of research, as it provides valuable qualitative information about the distribution of pressure and velocities in the flow. Various techniques for flow visualization were proposed, such as utilizing filaments, small light particles or coloured gas or smoke. WIth the progress in optical noncontact optical measurement techniques new possibilities arise for retrieving not only qualitative, but also quantitative data about flow behavior.

For exploiting the advantages of optical noncontact studying flow process at low velocities in hydrodynamic tunnel (Figure 1), the effect of light refraction at the boundaries of various optical media should be taken into account. The paper presents the developed technique for accurate 3D registration and visualization of flow during experiments in a hydrodynamic tunnel.

The main contributions of the study are:

(1) implementation of the developed techniques for accurate 3D measurements in multimedia optical working space in photogrammetric 3D measurement system;

(2) experimental 3D registration and 3D visualization of the flow jets in laboratory hydrodynamic tunnel;

(3) experimental evaluation of accuracy of multimedia 3D measurements for 3D visualization of the flow jets.

2 Related work

Visualization is playing an important role in scientific research, providing the best for analysis data representation. Visionbased methods for automatic generating accurate photorealistic 3D models of real objects of complicated shape [1, 2, 3, 4] or processes of complex nature and behaviour [5, 6, 7, 8] provide a new quality of data representation and, as a result, expand the possibilities of research efficiency. In aerodynamic and hydrodynamic flow visualization allows to exhibit the inner characteristics of the flow, that are essential for the process understanding.

Figure 1: Flow visualization in hydrodynamic tunnel

Etienne Jules Marey was the first who visualized and recorded air flow in the first wind tunnel [9]. Gustave Eiffel was a designer of this wind tunnel, that was installed at the foot of the Eiffel tower [10]. Marey proposed to inject into flow thin and parallel smoke jets, that can be recorded by photographic camera. Such invention allowed to analyze the direction of the flow and to retrieve information about the distribution of the velocities in different parts of the flow [11].

Many various techniques for flow visualization have been developed since the first experiments of Etienne Jules Marey. Among these there are visualisation with tufts, glued by one end to a model surface; generating air bubbles of small diameter, injected in the flow; techniques, based on registering variation in flow density, and interferometry methods. A detailed review of the modern flow visualization methods can be found in [10].

Addition of small highcontrast particles to flow is widely used for visualization and registration. Usually a system of high speed cameras working in synchronized mode register flow motion. Then the processing of these registrations are performed according either Eulerian or Lagrangian approach [12, 13, 14, 15]. Eulerian methods carry out voxelbased reconstruction of particles per time step, followed by 3D motion estimation, with some form of dense matching between the precomputed voxel grids from different time steps [16, 12].

Lagrangian techniques perform reconstructing an explicit sparse set of particles, the individual particles being tracked over time. Physical constraints can only be incorporated in a postprocessing step when interpolating the particle tracks to a dense motion field [13]. Some recent methods for object shape 3D reconstruction incorporate deep learning for multiview or even singleview 3D shape reconstruction [17, 18, 19, 20]. These methods look promising for further research in 3D flow analysis.

The impressive progress in visionbased 3D reconstruction methods allows accurate quantitative registration for further 3D visualization of flow process. The basis for accurate 3D measurements by optical system is an imaging model with correct parameters of system calibration. Calibration techniques, required for photogrammetric 3D measurements [21, 22], are mostly developed for the case of single optical environment, and for flow studying in a hydrodynamic tunnel they have to consider light refraction at optical media boundaries separating flow from optical measurement system.

Methods for calibration of optical systems for measurement in multimedia optical case can be roughly classified as follows. Some techniques target compensating distortion effects, that are caused by refraction. To exploit the effect of vanishing aberrations for light rays running through the optical interface at 90^o angle, special optical elements (such as prisms filled with water) are used [23]. Such technique is often applied in the case of fluid flow analysis using the methods of stereoscopic particle velocity measurements (PIV – particle image velocimetry) [24].

Another group of techniques account for the refraction in imaging model [25, 26, 27], and thus obtaining necessary accuracy of 3D measurements. To apply a modern photogrammetric workflow based on structurefrommotion and multiview stereo techniques [28] within existing software and workflow, refraction correction is applied at the photo level [29].

For some multimedia optical measurements applications an equitable approach is to “absorb” refraction effects by the estimated calibration parameters of the camera [30]. The approach is reasonable for the cases when the main effect of refraction is radially symmetric relative to the principal point. The “absorbing” technique gives appropriate description of the distortion model for the case of optical axis of the camera being close to perpendicular to the optical interface plane. Unfortunately, the method of “absorbing of refraction effects” always has some systematic errors, that are not accounted in the imaging model. The effect of refraction invalidates the assumption that the camera has a single center of projection [25, 31], which is the main assumption for such model.

To obtain a reliable and transparent method for accounting refraction effects, an accurate imaging model for the case of image acquisition through two optical media interfaces was developed [32]. It derives a set of equations, that directly describe the process of ray pass from a given object point to the image plane.

3 Experimental setup

The proposed technique for accurate flow 3D visualization is developed for flow behaviour analysis in hydrodynamic tunnel HDT400 of Central Aero and Hydrodynamic Institute (TsAGI). The HDT400 working space for placing scaled model of an aircraft or its wing is 400 × 400 ×400 mm. The workspace is available for monitoring the flow through glass walls. HDT400 has a vertical structure, and, being moved by gravity, water enters the working part of the tunnel from a water tank installed on top. The range of flow velocities in HDT400 is 2 . . . 10cm/s. The advantage of HDT400 hydrodynamic tunnel is possibility of studying aerodynamic process at velocities.

For preliminary technique study and testing a laboratory setup was created (Figure 2), that reconstruct study conditions of HDT400 hydrodynamic tunnel. It has vertical design similar HDT400 with a working part with dimensions 110 × 110 × 200 mm. A water tank is mounted above the working part, having a set of injectors for colozring flow jets during tests.

The common view of the laboratory setup is shown in Figure 2(a), and the working part with mounted stereolithography model of a wing is presented in Figure 2(b).

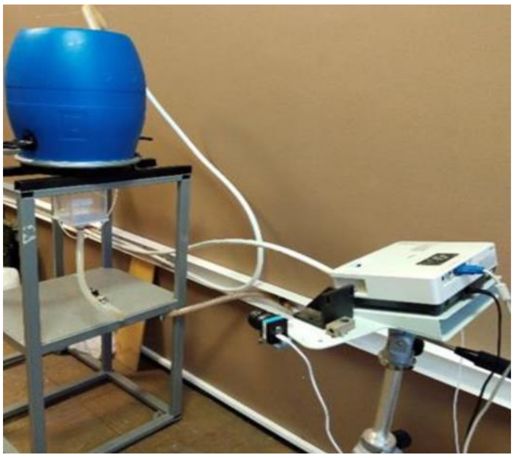

(a) Common view of the laboratory setup

(b) Working part with mounted stereolithography model of a wing and coloured jets

Figure 2: Laboratory setup for 3D visualization technique evaluating

The photogrammetric 3D reconstruction system “Mosca” [33] was used for 3D flow registration and accurate measurements. In laboratory setup the photogrammetric system “Mosca” in twocamera mode was used. For exploiting in optical multimedia conditions, “Mosca” photogrammetric software was extended to implement the developed algorithms, that account for refraction effects.

Table 1: DMK 37BUX273 camera specification

Parameter	Value
Sensor type	CMOS Pregius
Format	1/2.9”
Dynamic range	10 bit
Resolution	1, 440 × 1, 080
Pixel size	3.45 μm × 3.4 μm
Frame rate	up to 238 fps
Shutter	1μs to 30 s
Lens	6 mm

The optical 3D measurement system consists of two DMK 37BUX273 cameras equipped with the IMX273LLR Sony CMOS sensor, and Epson EMP1705 projector of structured light mounted on a rigid platform, providing stable exterior orientation. Main technical characteristics of the cameras are given in Table 1.

4 Algorithms for accounting refraction

For application in optical multimedia environment we modify the standard imaging model in form of collinearity equations to account for the refraction at optical media interfaces. Accurate imaging model [32] for this case consider refraction of light ray from an object point A to the corresponding image point a (Figure 3) at two optical interfaces: “airglass” and “glassliquid”.

The ray path for this case can be presented as three vectors $\mathbf{r^1}$, $\mathbf{r^2}$, $\mathbf{r^3}$ for air, for glass, and for liquid correspondingly.

Object Figure 3 presents the systems of coordinates, that are considered in the study. Coordinate system $OXYZ$ is related to studied object, image system of coordinates $Cxyz$ is related to the camera, and glass system of coordinates $\Omega X_g Y_g Z_g$ is related to glass wall of the working part.

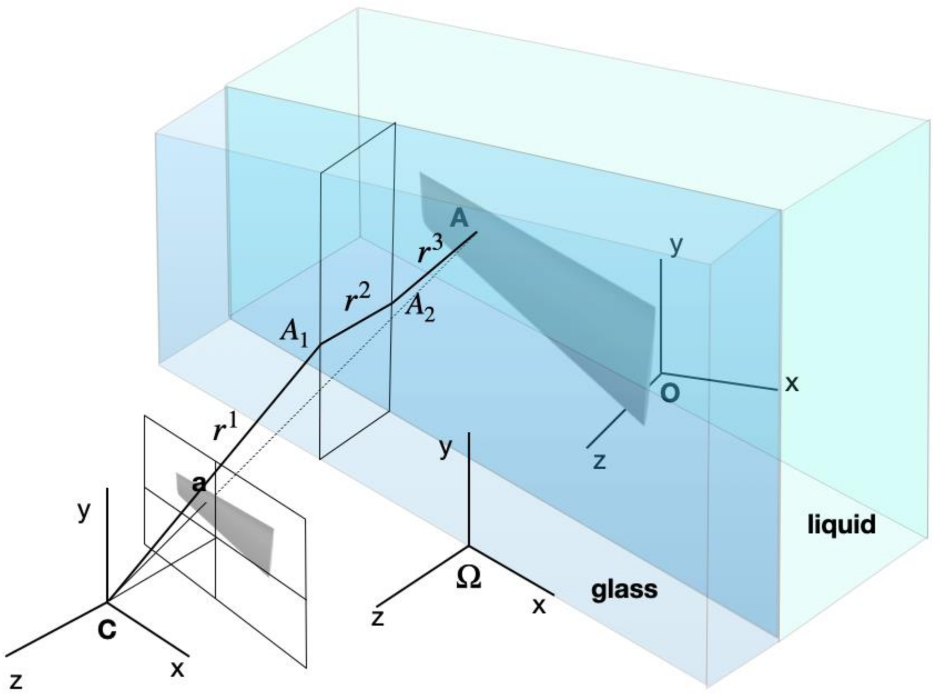

Figure 3: Systems of coordinates and the path of light ray.

For each vector $\mathbf{r^1}$, $\mathbf{r^2}$, $\mathbf{r^3}$ the equations defining its position in object coordinate system are derived using Snell law in form:

$$\mathbf{r^1} = \begin{pmatrix} X_1 \\ Y_1 \\ Z_1 \end{pmatrix} = \mathbf{R^T} \cdot \begin{pmatrix} x \\ y \\ -c \end{pmatrix} \tag{1}$$

$$\mathbf{r^2} = \begin{pmatrix} r_x^2 \\ r_y^2 \\ r_z^2 \end{pmatrix} = \begin{pmatrix} r_x^1 \cdot tg(\phi_2) \\ r_y^1 \cdot tg(\phi_2) \\ r_z^1 \end{pmatrix}, \ sin(\phi_2) = \frac{1}{n_1} \cdot sin(\phi_1) \tag{2}$$

$$\mathbf{r^3} = \begin{pmatrix} r_x^3 \\ r_y^3 \\ r_z^3 \end{pmatrix} = \begin{pmatrix} r_x^2 \cdot tg(\phi_3) \\ r_y^2 \cdot tg(\phi_3) \\ r_z^2 \end{pmatrix}, \ sin(\phi_3) = \frac{n_1}{n_2} \cdot sin(\phi_2) \tag{3}$$

The coordinates of origin of each vector C, A_1, A_2 are defined using parameters of camera exterior orientation and conditions of intersection with glass planes, the refraction indexes of glass n_1 and water n_2 are taken as known or determined during calibration [32]. The system of equations for light ray path from object point A to corresponding image point a can be written in form:

$$F(\boldsymbol{x}_a, n_1, n_2, \boldsymbol{X}_\Omega, \boldsymbol{X}_A - \boldsymbol{X}_C) = 0, \qquad (4)$$

The equation 4 establish the relations between object point $\boldsymbol{X}_A$, the center of projection $\boldsymbol{X}_C$, and image point $\boldsymbol{x}_a$. So it is some kind of analog of standard photogrammetric colnearity equations and can be used photogrammetric system calibration and object points 3D coordinates determination. The nonlinear distortion parameters are accounted as additional terms Δ_x, Δ_y in the equation 4. These terms are taken in form of BrownConrady model [34, 35]:

$$\Delta_x = a_0 \cdot y + x(a_1 r^2 + a_2 r^4 + a_3 r^6) + a_4(r^2 + 2x^2) + 2a_5 xy; \qquad (5)$$

$$\Delta_y = a_0 \cdot x + y(a_1 r^2 + a_2 r^4 + a_3 r^6) + a_5(r^2 + 2y^2) + 2a_4 xy; \qquad (6)$$

with $r^2 = x^2 + y^2$.

Here

x_a, y_a – coordinates of a point on the image,

$a_0, \ldots, a_5$ – camera interior orientation parameters:

a_0 – coefficient of affine distortion;

a_1, a_2, a_3 – coefficients of radial distortion;

a_4, a_5 – coefficients of tangential distortion.

The vector $\boldsymbol{v}_e^l = (x_p, y_p, m_x, m_y, a_0, \ldots, a_5)^T$ of interior orientation parameters is estimated by calibration procedure [32]. $\boldsymbol{v}_e^l$ includes coordinates of principal point, image scales and additional parameters correspondingly, spatial coordinates of reference points being known by independent precise measurements. The unknown parameters are determined by least mean square estimation using image coordinates of a set of the test field reference points as observations [36, 37].

Table 2: Interior orientation parameters

Parameter	Calibration parameters			
	calibration stand		hydrodynamic tunnel	
m_x, mm	0,00343588	0,003437963	0,00343612	0,00343903
m_y, mm	0,00343487	0,003437819	0,00343516	0,00343804
x_p, pix	742,12	760,87	734,77	740,07
y_p, pix	587,22	578,64	618,09	555,33
a_0	-0,0005583931	-0,0004862325	-0,0005524741	-0,0005100927
a_1	0,0120703300	0,0116045100	0,0112192311	0,0119018751
a_2	0,0004580167	0,0003427741	0,0004681763	0,0003358998
a_3	-0,0000339890	-0,0000381674	-0,0000330094	-0,0000401097
a_4	-0,0000171022	-0,0001142789	-0,0000165125	-0,0001193499
a_5	0,0001381050	-0,0001101241	0,0001424769	-0,0001050232

5 Experimental results

The laboratory setup was used to evaluate the developed technique. Firstly, evaluation of the calibration technique for the optical multimedia case was performed. The results of the estimation of the interior orientation parameters at the laboratory hydrodynamic tunnel were compared with results of the calibration at the special multimedia calibration stand [38]. Table 2 presents results of the calibration for both cases, demonstrating good correspondence of two different calibrations.

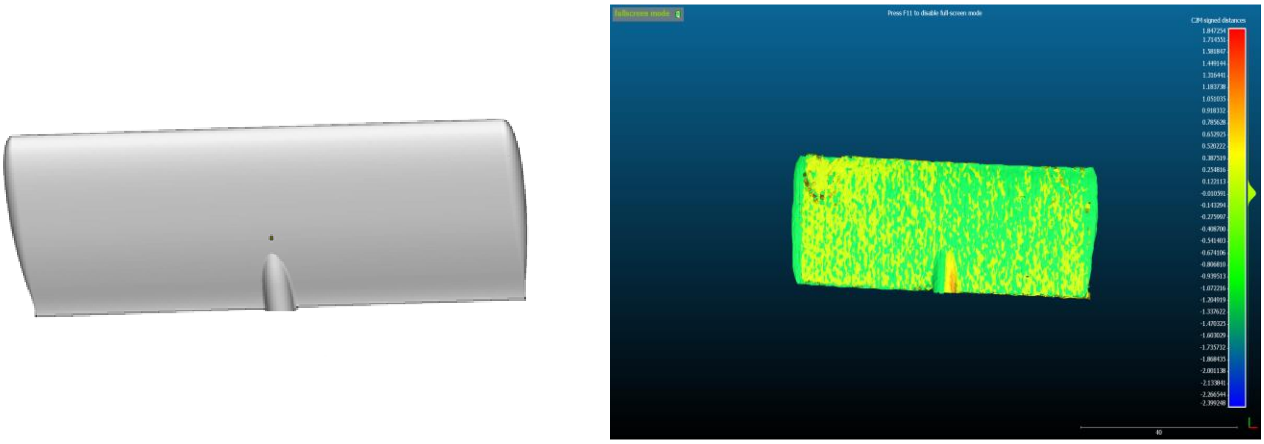

(a) CADmodel of the wing used for 3D printing

(b) Comparison of 3D scan with CADmodel used for 3D printing

Figure 4: Results of measurement comparison

To obtain another kind of estimation of the accuracy of 3D measurements, experimental 3D scanning of a reference object was carried out. Wing stereolithography (SLA) model (Figure 4(a)) designed for experiments in the hydrodynamic tunnel was used as the reference object, and 3D scanning was performed for SLAmodel placed in working part of laboratory hydrodynamic tunnel. The result of comparison CADmodel of the wing with 3D scan of the SLAmodel is shown in Figure 4(b). *CloudCompare* software[1] was used to match and to compare 3D model. *CloudCompare* is open source software developed for 3D point cloud and mesh processing, alignment and comparison.

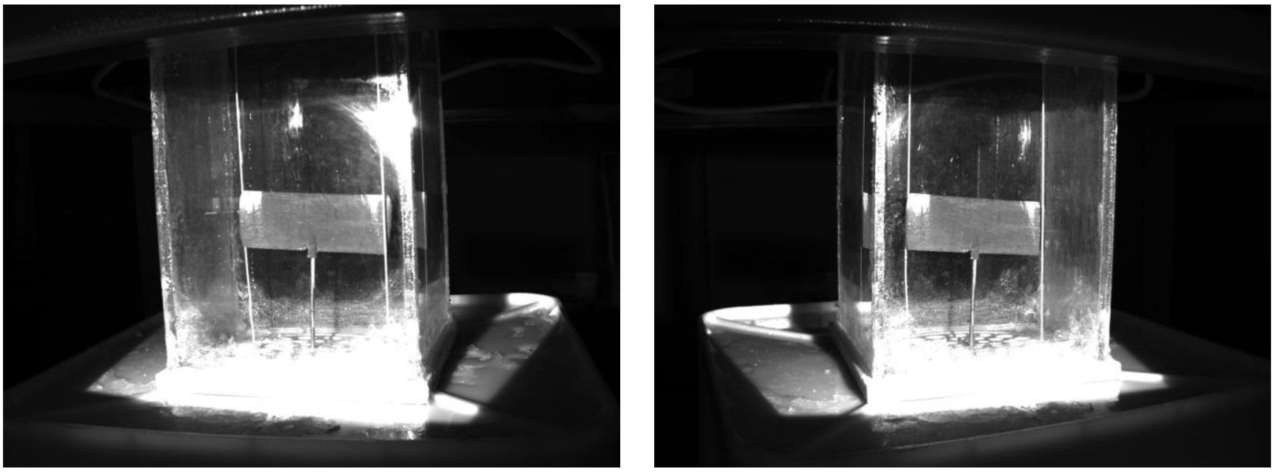

(a) Stereo pair of the flow in the working part of the laboratory setup

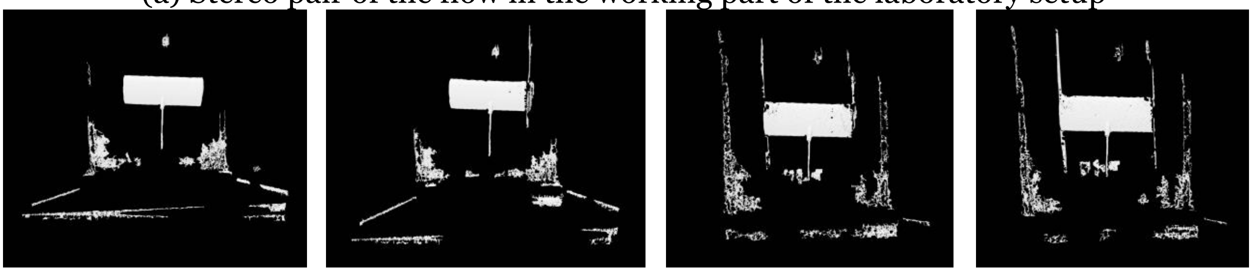

(b) A time series of 3D reconstructions of flow in working part of the laboratory setup

Figure 5: Stereo pair of the flow and 3D reconstruction of flow in the working part of the laboratory setup

[1] https://www.cloudcompare.org

In Figure 4b we can see a high level of correspondence between surface 3D reconstruction in multi media case corresponds and CADmodel, mean error between surfaces being about 0.03 *mm*.

The second stage of experimental evaluation was aimed at 3D registration, 3D reconstruction and 3D visualization of flow jets at the laboratory hydrodynamic tunnel. Figure 5 shows a stereo pair of images from left and right cameras and the results of flow jets 3D reconstruction.

Combined 3D scanningjet detection technique was applied for 3D reconstruction and 3D visualisation of flow jets. 3D scanning allows reconstructing the working part of the laboratory hydrodynamic tunnel with the SLAmodel of a wing, installed there. 3D reconstruction of flow jets was carried out with jets detection algorithm. For robust jets detection in the image, preliminary acquired images of the hydrodynamic tunnel working part were used for separating background from jets images. Then detects jets were reconstructed by photogrammetric technique.

Figure 5(b) demonstrates several frames from a sequence of flow jets 3D registration. The developed technique allows to visualize and to analyze the 3D evolution of flow jets in time.

6 Conclusion

The technique for accurate 3D visualization of the flow motion in a hydrodynamic tunnel has been developed. The basis for an accurate 3D reconstruction of the shape of the stream jets is the calibration of the photogrammetric motion capture system using a developed image formation model that takes into account refraction at the interface of optical media.

Experimental evaluation of the developed technique using a laboratory hydrodynamic tunnel shows high accuracy of 3D measurements for spatiotemporal visualization of the flow. The developed technique provides accurate 3D visualization of flow jets in time, thus allowing to analyze the 3D evolution of the flow. The experiments proved the applicability of the developed techniques of optical system calibration and flow motion 3D visualization for exploiting in aircraft icing study.

Acknowledgments

The reported study was supported by Russian Foundation for Basic Research (RFBR) according to the research project 19-29-13040.

References

[1] Eker, R., Elvanoglu, N., Ucar, Z., Bilici, E., Aydın, A.: 3d modelling of a historic windmill: Ppkaided terrestrial photogrammetry vs smartphone app. The International Archives of the Photogrammetry, Remote Sensing and Spatial Information Sciences XLIIIB22022, 787–792 (2022), https://www.intarchphotogrammremotesensspatialinfsci.net/XLIIIB22022/787/2022/

[2] Girelli, V.A., Tini, M.A., D'Apuzzo, M.G., Bitelli, G.: 3d digitisation in cul tural heritage knowledge and preservation: The case of the neptune statue in bologna and its archetype. The International Archives of the Photogram Remote Sensing and Spatial Information Sciences XLIIIB22020, 1403–metry, 1408 (2020), https://www.intarchphotogrammremotesensspatialinfsci.net/XLIIIB22020/1403/2020/

[3] Knyaz, V.A., Kniaz, V.V., Remondino, F., Zheltov, S.Y., Gruen, A.: 3d reconstruction of a complex grid structure combining uas images and deep learning. Remote Sensing 12(19), 3128 (Sep 2020), http://dx.doi.org/10.3390/rs12193128

[4] Andreev, S.V., Bondarev, A.E., Bondarenko, A.V., Vizilter, Y.V., Galaktionov, V.A., Gudkov, A.V., Zheltov, S.Y., Zhukov, V.T., Ilovayskaya, E.B., Knyaz, V.A., Manukovsky, K.V., Novikova, N.D., Ososkov, M.V., Silaev, N.Z., Feodoritova, O.B., Bondareva, N.A.: Modelling and visualisation of blade assembly with complicated shape for power turbine. Scientific Visualization 7(4) (2015)

[5] Lin, J., Foucaut, J.M., Laval, J.P., P´erenne, N., Stanislas, M.: Assessment of Different SPIV Processing Methods for an Application to NearWall Turbulence, pp. 191–221. Springer Berlin Heidelberg, Berlin, Heidelberg (2008), https://doi.org/10.1007/ 978354073528110

[6] Kniaz, V.V.: Fast instantaneous center of rotation estimation algorithm for a skied-steered robot. In: Remondino, F., Shortis, M.R. (eds.) Videometrics, Range Imaging, and Applications XIII. vol. 9528, pp. 194 – 204. International Society for Optics and Photonics, SPIE (2015), https://doi.org/10.1117/12.2184834

[7] Chatzitofis, A., Albanis, G., Zioulis, N., Thermos, S.: A lowcost & realtime motion capture system. In: Proceedings of the IEEE/CVF Conference on Computer Vision and Pattern Recognition (CVPR). pp. 21453–21458 (June 2022)

[8] Kniaz, V.V.: Robust visionbased pose estimation algorithm for an uav with known gravity vector. The International Archives of the Photogrammetry, Remote Sensing and Spatial Information Sciences XLIB5, 63–68 (2016), https://www.intarchphotogrammremotesensspatialinfsci.net/XLIB5/63/2016/

[9] Des mouvements de l'air lorsqu'il rencontre des surfaces de diff´erentes formes. Comptes rendus hebdomadaires des s´eances de l'Acad´emie des sciences 131, 160–163 (1900)

[10] Chanetz, B., D´elery, J., Gilli´eron, P., Gnemmi, P., Gowree, E.R., Perrier, P.: Flow Visualisation Techniques, pp. 165–182. Springer International Publishing, Cham (2020), https://doi.org/10.1007/97830303556237

[11] Fermigier, M.: The use of images in fluid mechanics. Comptes Rendus M´ecanique 345(9), 595–604 (2017), https://www.sciencedirect.com/science/article/pii/ S1631072117300918, a century of fluid mechanics: 1870–1970

[12] Lasinger, K., Vogel, C., Schindler, K.: Volumetric flow estimation for incompressible fluids using the stationary stokes equations. In: 2017 IEEE International Conference on Computer Vision (ICCV). pp. 2584–2592 (Oct 2017)

[13] Schanz, D., Gesemann, S., Schr¨oder, A.: Shakethebox: Lagrangian particle tracking at high particle image densities. Experiments in Fluids 57(5), 70 (2016), https://doi.org/ 10.1007/s0034801621571

[14] Lasinger, K., Vogel, C., Pock, T., Schindler, K.: 3d fluid flow estimation with integrated particle reconstruction. International Journal of Computer Vision 128(4), 1012–1027 (2020), https://doi.org/10.1007/s11263019012616

[15] Rubbert, A., Schr¨oder, W.: Iterative particle matching for threedimensional particle tracking velocimetrys. Experiments in Fluids 61(2), https://doi.org/10.1007/s003480202891258 (2020)

[16] Barbu, I., Herzet, C., M´emin, E.: Joint Estimation of Volume and Velocity in TomoPIV. In: 10TH INTERNATIONAL SYMPOSIUM ON PARTICLE IMAGE VELOCIMETRY PIV13. p. 45. Delft, Netherlands (Jul 2013), https://hal.archivesouvertes.fr/ hal00880712

[17] Huang, Q., Wang, H., Koltun, V.: Singleview reconstruction via joint analysis of image and shape collections. ACM Trans. Graph. 34(4) (Jul 2015), https://doi.org/10.1145/ 2766890

[18] Roth, S., Richter, S.R.: Matryoshka networks: Predicting 3d geometry via nested shape layers. In: 2018 IEEE/CVF Conference on Computer Vision and Pattern Recognition. pp. 1936–1944 (June 2018)

[19] Kniaz, V.V., Remondino, F., Knyaz, V.A.: Generative adversarial networks for single photo 3d reconstruction. ISPRS International Archives of the Photogrammetry, Remote Sensing and Spatial Information Sciences XLII2/W9, 403–408 (2019), https://www.intarchphotogrammremotesensspatialinfsci.net/XLII2W9/403/2019/

[20] Knyaz, V.: Machine learning for scene 3d reconstruction using a single image. Proc. SPIE 11353, Optics, Photonics and Digital Technologies for Imaging Applications VI 11353, 1135321 (2020), https://doi.org/10.1117/12.2556122

[21] Remondino, F., Fraser, C.: Digital camera calibration methods: Considerations and comparisons. ISPRS International Archives of the Photogrammetry, Remote Sensing and Spatial Information Sciences XXXVI5, 266–272 (September 2006)

[22] Vo, M.N., Wang, Z., Luu, L., Ma, J.: Advanced geometric camera calibration for machine vision. Optical Engineering 50(11), 1 – 4 (2011), https://doi.org/10.1117/1.3647521

[23] Raffel, M., Willert, C.E., Scarano, F., K¨ahler, C.J., Wereley, S.T., Kompenhans, J.: Stereoscopic PIV, pp. 285–307. Springer International Publishing, Cham (2018), https: //doi.org/10.1007/9783319688527{_}8

[24] Teich, M., Grottke, J., Radner, H., Buttner, L., Czarske, J.W.: Adaptive particle image velocimetry based on sharpness metrics. J. Eur. Opt. Soc.Rapid Publ. 14(5) (2018), https://jeos.springeropen.com/articles/10.1186/s4147601800730

[25] Sedlazeck, A., Koch, R.: Perspective and nonperspective camera models in underwater imaging – overview and error analysis. In: Dellaert, F., Frahm, J.M., Pollefeys, M., Leal-Taix´e, L., Rosenhahn, B. (eds.) Outdoor and LargeScale RealWorld Scene Analysis. pp. 212–242. Springer Berlin Heidelberg, Berlin, Heidelberg (2012)

[26] Murase, T., Tanaka, M., Tani, T., Miyashita, Y., Ohkawa, N., Ishiguro, S., Suzuki, Y., Kayanne, H., Yamano, H.: A photogrammetric correction procedure for light refraction effects at a twomedium boundary. Photogrammetric Engineering and Remote Sensing 74(9), 1129–1136 (2008), http://www.documentation.ird.fr/hor/{PAR}00002751

[27] Gonz´alezVera, A.S., Wilting, T.J.S., Holten, A.P.C., van Heijst, G.J.F., DuranMatute, M.: Highresolution singlecamera photogrammetry: incorporation of refraction at a fluid interface. Exp Fluids 61(3) (2020), https://doi.org/10.1007/s003480192826y

[28] Knyaz, V., Zheltov, S.: Accuracy evaluation of structure from motion surface 3D reconstruction. In: Remondino, F., Shortis, M.R. (eds.) Videometrics, Range Imaging, and Applications XIV. vol. 10332, pp. 200 – 209. International Society for Optics and Photonics, SPIE (2017), https://doi.org/10.1117/12.2272021

[29] Skarlatos, D., Agrafiotis, P.: A novel iterative water refraction correction algorithm for use in structure from motion photogrammetric pipeline. Journal of Marine Science and Engineering 6(3) (2018), https://www.mdpi.com/20771312/6/3/77

[30] Menna, F., Nocerino, E., Fassi, F., Remondino, F.: Geometric and optic characterization of a hemispherical dome port for underwater photogrammetry. Sensors 16(1) (2016), https: //www.mdpi.com/14248220/16/1/48

[31] Chadebecq, F., Chadebecq, F., Vasconcelos, F., Lacher, R., Maneas, E., Desjardins, A., Ourselin, S., Vercauteren, T., Stoyanov, D.: Refractive twoview reconstruction for under water 3d vision. International Journal of Computer Vision (2019), https://doi.org/10.1007/s11263019012189

[32] Knyaz, V.A., Stepaniants, D.G., Tsareva, O.: Optical system calibration for 3d measurements in hydrodynamic tunnel. Computer Optics 45(1), 58–65 (2021), http://computeroptics.ru

[33] Knyaz, V.A.: Scalable photogrammetric motion capture system "mosca": Development and application. ISPRS International Archives of the Photogrammetry, Remote Sensing and Spatial Information Sciences XL5/W6, 43–49 (May 2015), https://www.intarchphotogrammremotesensspatialinfsci.net/XL5W6/43/2015/

[34] Brown, D.: Decentering distortion of lenses. Photogrammetric Engineering 32(3), 444–462 (1966)

[35] Beyer, H.: Advances in characterization and calibration of digital imaging systems. Int. Arch. Photogramm. Remote Sens. Spatial Inf. Sci. XXIX, 545–555 (1992)

[36] Knyaz, V.A.: Automated calibration technique for photogrammetric system based on a multimedia projector and a ccd camera. ISPRS International Archives of the Photogrammetry, Remote Sensing and Spatial Information Sciences XXXVI5, 1–5 (2006), https://www.isprs.org/proceedings/XXXVI/part5/

[37] Kniaz, V.V., Grodzitskiy, L., Knyaz, V.A.: Deep learning for coded target detection. The International Archives of the Photogrammetry, Remote Sensing and Spatial Information

Sciences XLIV2/W12021, 125–130 (2021), https://www.intarchphotogrammremotesensspatialinfsci.net/XLIV2W12021/125/2021/

[38] Knyaz, V.A., Ippolitov, E.V., Novikov, M.M.: Accuracy assessment of optical 3D measure ments in hydrodynamic tunnel. In: Lehmann, P., Osten, W., Jr., A.A.G. (eds.) Optical Measurement Systems for Industrial Inspection XII. vol. 11782, pp. 326 – 336. International Society for Optics and Photonics, SPIE (2021), https://doi.org/10.1117/12.2592622